Chinese Journal of
POLYMER SCIENCE

RESEARCH ARTICLE

https://doi.org/10.1007/s10118-025-3373-z
Chinese J. Polym. Sci. **2025**, *43*, 1584–1591

Transparent and Flexible Surface-enhanced Raman Scattering (SERS) Substrates with High SERS Performance and Stability

Jian-Ping Peng[a,†], Pei-Jiang Liu[c,†], Yu-Tao Song[a], Shan-Zheng Zhao[a], Xin-Yue Deng[b], and Zhen-Kai Huang[b*]

[a] *School of Environment and Chemical Engineering, Foshan University, Foshan 528000, China*
[b] *School of Materials and Energy, Foshan University, Foshan 528000, China*
[c] *Reliability Physics and Application Technology of Electronic Component Key Laboratory, the 5th Electronics Research Institute of the Ministry of Industry and Information Technology, Guangzhou 510610, China*

Electronic Supplementary Information

Abstract This paper presents a polymer-brush-guided templating strategy for fabricating ordered gold plasmonic architectures. The synthesized nanostructures featuring densely packed Au nanoparticles (NPs) exhibited strong surface-enhanced Raman scattering (SERS) activity. Using a simple mechanical transfer technique, these assemblies were integrated into flexible polydimethylsiloxane (PDMS) films. Polymer encapsulation during synthesis ensures structural integrity during processing, resulting in a mechanically robust SERS substrate with exceptional analytical performance. This platform achieved 4-mercaptobenzoic acid (4-MBA) detection at 100 pmol/L (10^{-10} mol/L) with high reproducibility (RSD=6.8%). Environmental and mechanical stability tests demonstrated 95% signal retention over 30 days and sustained functionality after 100 bending/twisting cycles. Combined with a non-destructive adhesion-transfer protocol, the substrate enabled on-site thiram detection on apple surfaces (1 μmol/L limit). This study provides a scalable approach for developing flexible SERS devices for food safety monitoring and environmental analysis.

Keywords Flexible sensors; Patterned Au nanostructures; Polydimethylsiloxane; Surface-enhanced Raman scattering

Citation: Peng, J. P.; Liu, P. J.; Song, Y. T.; Zhao, S. Z.; Deng, X. Y.; Huang, Z. K. Transparent and flexible surface-enhanced raman scattering (SERS) substrates with high SERS performance and stability. *Chinese J. Polym. Sci.* **2025**, *43*, 1584–1591.

INTRODUCTION

As the population grows and agricultural production expands, organic pesticides are increasingly being used to control plant diseases and insect pests. However, excessive pesticide residues in the soil, fruits, and vegetables pose a serious threat to human health.[1] Therefore, there is a need for a simple and effective method to detect pesticide residues.[2] Traditional chromatographic methods are accurate, but require expensive equipment and complex pretreatment procedures. Surface-enhanced Raman scattering (SERS) has emerged as a highly sensitive analytical tool with broad applications in biomedical research, chemical analyses, and clinical diagnostics.[3–5] The remarkable signal amplification in surface-enhanced Raman scattering (SERS) arises from localized surface plasmon resonance (LSPR), a phenomenon in which collective electron oscillations in metallic nanostructures intensify Raman signals by several orders of magnitude. These nanoscale regions of extreme electromagnetic field enhancement, commonly termed "hot spots,"[6–9] enable ultrasensitive molecular detection. Compared with conventional chromatographic techniques that require complex instrumentation, SERS provides a rapid, field-deployable alternative for pesticide residue analysis in agricultural products.

In recent decades, efforts have been made to develop sophisticated SERS substrates for non-destructive and sensitive analysis of food contaminants. Conventional rigid substrates such as silicon wafers-, glass-, and metal-based platforms with uniformly and densely packed "hot spots" have been developed.[10,11] However, their lack of flexibility limits their use in the detection of analytes on curved objects.[12] Flexible SERS substrates such as paper-,[13,14] polymer-,[15] and carbon-based platforms[16,17] have attracted interest because of their adaptability to practical applications.[18,19] Despite the fabrication of many flexible SERS substrates for detecting pesticide residues in vegetable and fruit peels through a "press-peel off" process, challenges remain.[20–22] For example, a common preparation method for flexible SERS substrates involves the physical deposition of noble metal nanostructures on the surface of flexible platforms, where the nanostructures and platforms are connected through van der Waals forces.[23,24] The low adhesion between metal nanostructures and flexible platforms can cause the fall of metal nanostructures during mechanical deformations and sampling processes, reducing the number of "hot spots" and decreasing Ra-

* Corresponding author, E-mail: hzk@fosu.edu.cn
† These authors contributed equally to this work.
Received April 7, 2025; Accepted May 2, 2025; Published online July 1, 2025

man homogeneity and sensitivity. Moreover, for good adhesion, nanostructures have been encased in flexible substrates such as polyvinyl alcohol (PVA) hydrogels or polydimethylsiloxane (PDMS) films,[25,26] which have achieved better stability and durability of flexible SERS substrates to some extent. How ever, the distance between the probe molecules and the nanostructures in PVA hydrogels or PDMS films is not sufficiently small to achieve the best Raman scattering of the SERS substrates. Therefore, developing a method for fabricating flexible SERS substrates with good Raman enhancement and high sensitivity is of great significance.

In this study, we present a simple and robust method for preparing flexible SERS sensors with high sensitivity and stability for trace detection. Patterned Au nanostructures grown on silicon wafers using a polymer brush templated synthesis strategy (see Fig. 1a and Figs. S1–S5 in the electronic supple-

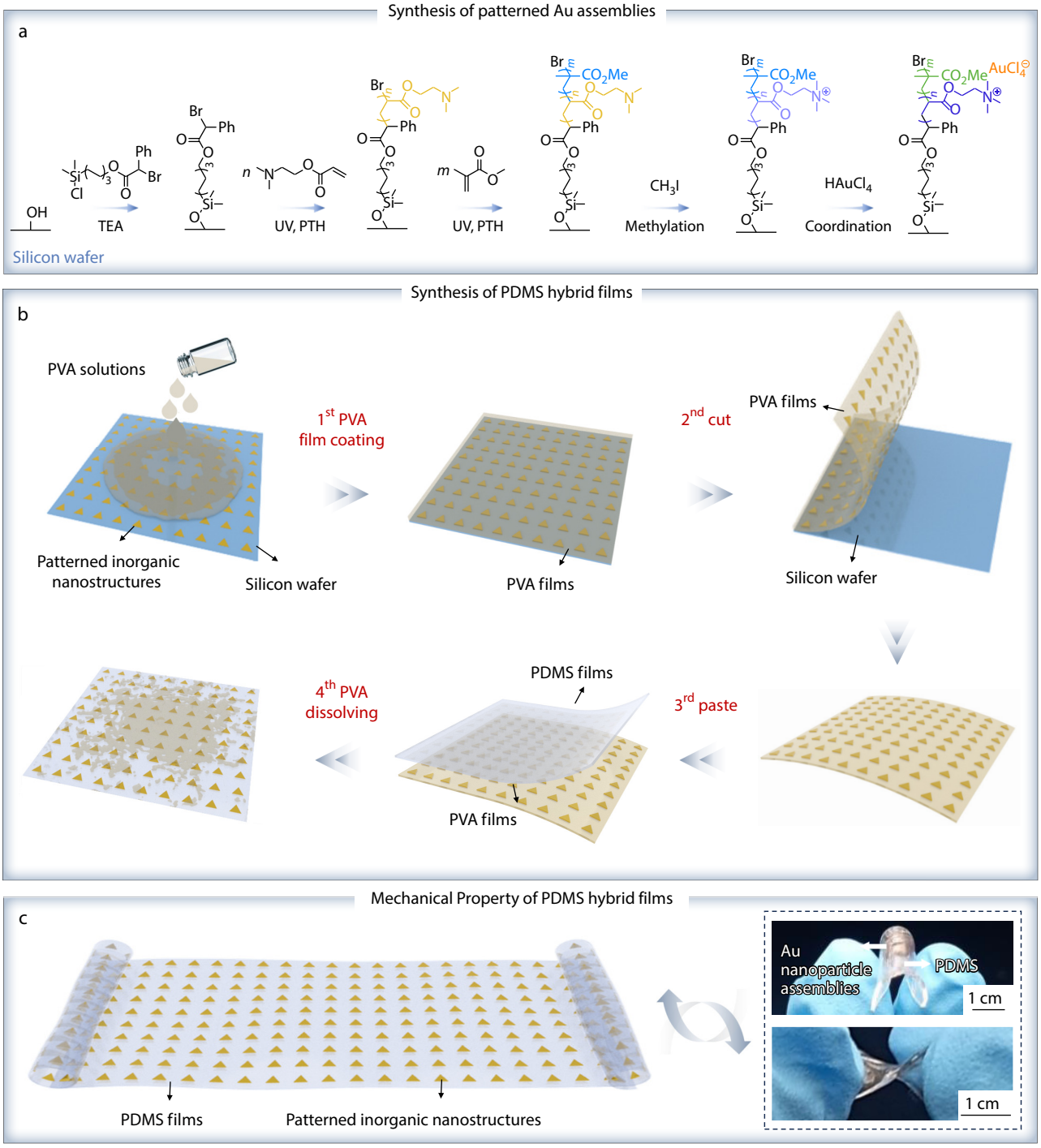

Fig. 1 (a) Schematic illustration of the *in situ* synthesis of patterned Au NP assemblies; (b) Schematic illustration of the PDMS hybrid films by simple "cut-and-paste" procedure; (c) Flexible PDMS provides excellent bending and twisting resistance for the SERS substrates.

https://doi.org/10.1007/s10118-025-3373-z

mentary information (ESI) for the experimental setup)[27,28] were transferred to PDMS thin films through a simple "cut-and-paste" procedure (Fig. 1b). The templating strategy utilizing polymer brushes enabled precise regulation of Au nanoparticle (NP) the dimensions and morphologies, composed of densely packed Au NPs attached to the silicon wafer *via* encapsulated polymer chains.[27,28] Therefore, the Au NP architectures retained their structural fidelity even when subjected to mechanical "cut-and-paste" transfer operations and showed good mechanical stability after being transferred to PDMS films because of the encapsulation of polymer templates. In particular, the flexible nature of the PDMS film allows the flexible SERS substrate to bend and twist while maintaining its functional stability (Fig. 1c). The massive electromagnetic "hot spots" among the closely packed Au NPs enabled the flexible films to have enormous SERS effects and capability for practical analysis of pesticide residues. This study provides a simple and robust method for fabricating flexible SERS substrates with good sensitivity and mechanical stability for practical detection applications.

EXPERIMENTAL

The preparation process is schematically illustrated in Fig. 1(a) and experimental details are summarized in the ESI.[27,28] Patterned polymethacryloyloxyethyl trimethylammonium chloride-block-poly(methyl methacrylate) (PMETAC-*b*-PMMA) block copolymer brushes were fabricated on silicon substrates through photoinduced surface-initiated atom transfer radical polymerization combined with photomask patterning. The cationic PMETAC domains functioned as spatially confined reaction chambers for gold precursor immobilization, facilitated by electrostatic and coordination interactions between quaternary ammonium groups and $[AuCl_4]^-$ complexes. Subsequent *in situ* reduction within these hydrophilic domains yielded organized gold nanoparticle assemblies, while the hydrophobic PMMA matrix formed a protective surface layer over the nanostructured arrays. This hierarchical fabrication strategy enables precise spatial control over plasmonic nanostructure formation.

Subsequently, a PVA solution was applied to silicon-supported nanostructures and thermally cured to form a composite film. The PVA-nanostructure assembly was transferred onto a partially cured PDMS substrate, followed by secondary thermal curing to achieve structural fixation. Subsequent solvent immersion selectively removed the sacrificial PVA layer, enabling precise transfer of the patterned gold nanostructures onto the PDMS matrix (detailed protocols provided in ESI). This interfacial engineering strategy successfully yields transparent, mechanically compliant SERS substrates while preserving the integrity and spatial organization of the plasmonic nanoarchitectures.

RESULTS AND DISCUSSION

In this study, we selected PDMS as the substrate for flexible SERS because of its favorable processing characteristics and flexibility, which are superior to those of other materials utilized in flexible SERS substrates such as PVA.[29] Additionally, PDMS exhibits enhanced water resistance compared with other materials. As shown in Fig. 2(a), the colorless PDMS film turned lavender after the attachment of the patterned Au plasmonic nanostructures. Triangular Au nanostructures with geometric uniformity (edge length: 20 μm; thickness: 33±7 nm) were successfully synthesized, as confirmed by microscopic analysis (Fig. 2b). The optical microscope image (Fig. 2c) further confirms the formation of the patterned Au NP assemblies-PDMS hybrid film. We observed the microstructure of an individual triangular nanosheet in a flexible SERS substrate using atomic force microscopy (AFM) (Fig. 2d). As can be seen from the AFM height data, the triangular nanosheet has a flat top surface with a thickness of approximately 25 nm (Fig. 2e), which is thin and flat relative to the 20 μm lateral size of the nanosheet.

Prior to TEM characterization, the Au NP architectures were delaminated from the silicon substrates through mechanical exfoliation (experimental details are provided in the ESI). As shown in Fig. 2(f), the triangular morphology was preserved post-delamination, a structural resilience resulting from in situ polymer encapsulation during NP synthesis.[30,31] This protective interaction effectively maintained assembly integrity throughout the transfer process. FE-SEM imaging (Fig. 2g) revealed a homogeneous Au NP distribution across the PDMS surfaces, confirming dense packing without aggregation. Complementary structural analyses, including HR-TEM lattice imaging, SAED crystallography, and GI-WAXD profiling (Figs. 2h, 2i and Fig. S6 in ESI) collectively verified the polycrystalline nature and spatial uniformity of the nanoparticle assemblies.

The flexible SERS substrate was immersed in a solution of 4-mercaptobenzoic acid (4-MBA) for different time to investigate the effect of immersion time on the response signal intensity (Fig. 3a). The experimental results show that the SERS response signal first increases rapidly with increasing immersion time and then tends to be constant for 120 min. The difference between the SERS signal intensities generated by 60 and 120 min of immersion was no longer significant. Therefore, we believe that 60 min of immersion is sufficient for this SERS substrate. To explore the limit of detection (LOD) of the PDMS-based SERS substrates, the correlation between the Raman signal intensity and the concentrations of 4-MBA aqueous ranging from 1 μmol/L to 100 pmol/L (10^{-6}–10^{-10} mol/L) was studied (Fig. 3b). Characteristic Raman vibrational modes corresponding to C—S stretching (1078 cm^{-1}) and aromatic ring deformation (1586 cm^{-1}) were consistently detected across all analyte concentrations, with signal attenuation correlating linearly with reduced 4-MBA concentrations. The PDMS-supported Au NP assemblies demonstrated exceptional analytical sensitivity, as evidenced by a 100 pmol/L (10^{-10} mol/L) detection threshold, confirming their efficacy as high-performance SERS-active platforms. Choosing the 1078 cm^{-1} peak as the analytical readout, we acquired the calibration curve of 4-MBA identification, and the result showed a linear dependence of the Raman peak intensity on the concentration of 4-MBA molecules (R^2 = 0.950), which suggests the potential for quantitative detection of probe molecules at trace concentrations (Fig. 3c).

The SERS enhancement magnitude was quantitatively assessed by calculating the surface-averaged enhancement factor (EF). The optimized substrate exhibited an EF value of 1.76×10^8 (see ESI), primarily driven by intensive plasmonic cou-

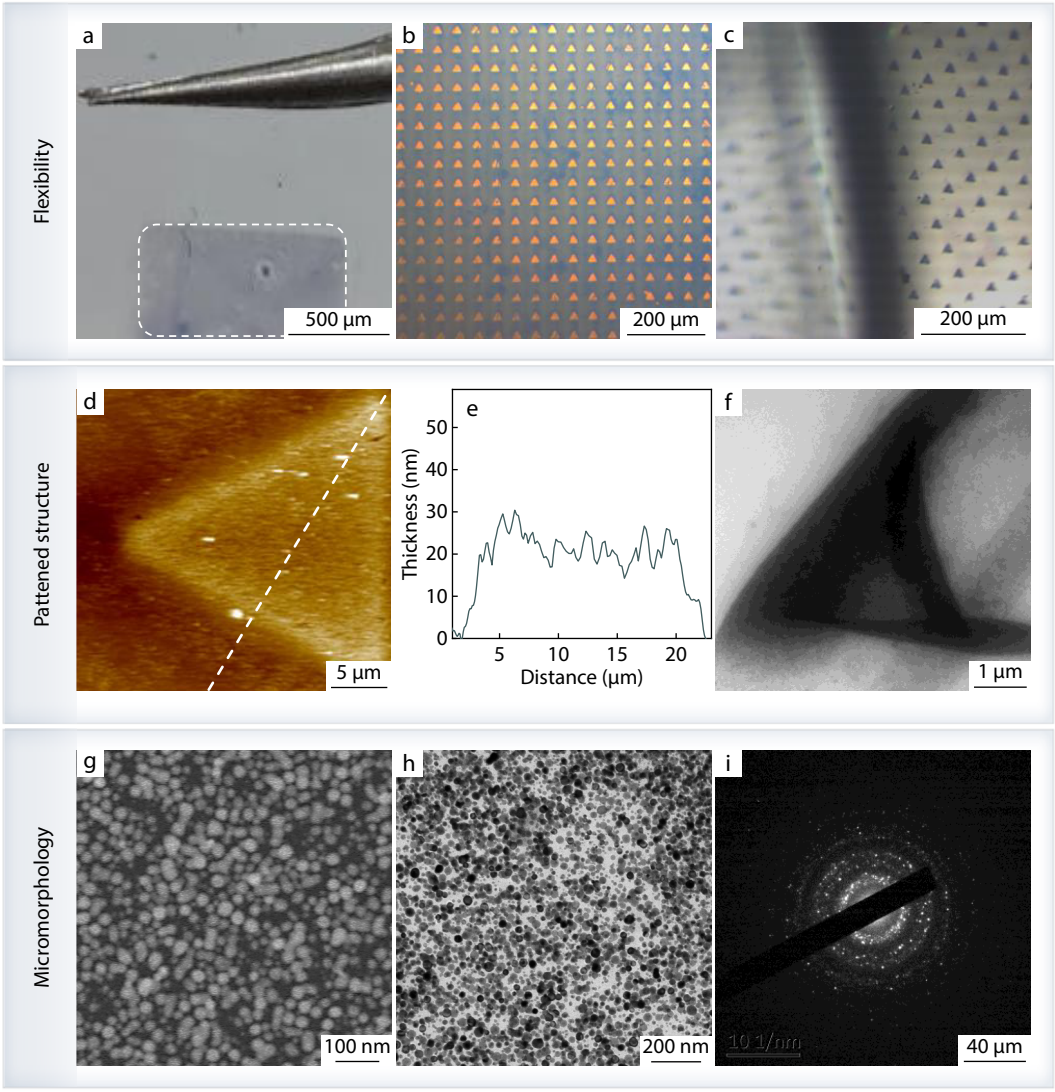

Fig. 2 (a) Optical microscope image of triangular Au nanostructures before being transferred to PDMS; (b) Low- and (c) high-magnification optical microscope image of the PDMS-based SERS substrate; (d) AFM analysis of the Au nanostructure and (e) its thickness after the removal of outer PMMA layer; (f) TEM image of the triangular Au NP assemblies; (g) High- and (h) low-magnification TEM, and (i) the corresponding SAED images of the triangular Au NP assemblies after peeling-off from the silicon wafer.

pling at interparticle nanogaps within the densely packed Au NP arrays. To evaluate the spatial uniformity, grid-based mapping across 20 predefined sites revealed minimal signal variation (6.8% RSD, Figs. 3d and 3e), confirming exceptional homogeneity for trace analyte detection. This performance aligns with our earlier findings[27,28] regarding the pattern-induced stabilization of SERS-active architectures. Mechanistic analysis suggests that the controlled mass transport kinetics during the redox process govern the nucleation and growth of Au NPs within the polymer matrix. Specifically, confined ion diffusion along patterned brush edges promoted a uniform NP distribution, whereas non-patterned regions exhibited accelerated diffusion near structural imperfections, leading to heterogeneous growth.

To assess the long-term stability, the hybrid PDMS films were subjected to ambient storage conditions with periodic SERS signal monitoring at five-day intervals. As shown in Fig. 3(f), the Raman intensities exhibited only minor variations after a period of storage, further verifying the excellent stability of the flexible SERS substrate. To further confirm the state of the Au NPs in the substrate, XRD analysis was performed on the Au NPs embedded in the flexible substrate (Fig. S7 in ESI). The experimental results confirmed the face-centered cubic crystal structure of the Au NPs, with characteristic peaks observed at 38.2°, 44.4°, and 64.6° corresponding to the (111), (200), and (220) crystallographic planes, respectively. Additionally, no peaks associated with Au oxides (*e.g.*, Au_2O_3) were detected, indicating that the NPs remained in a metallic state under the synthesis and storage conditions employed in this study. Therefore, the stability of the Au NPs encapsulated within the polymer brushes provided a flexible substrate with adequate durability. Consequently, the PDMS hybrid films stored in air for a certain period could still exhibit consistent SERS effects.

https://doi.org/10.1007/s10118-025-3373-z

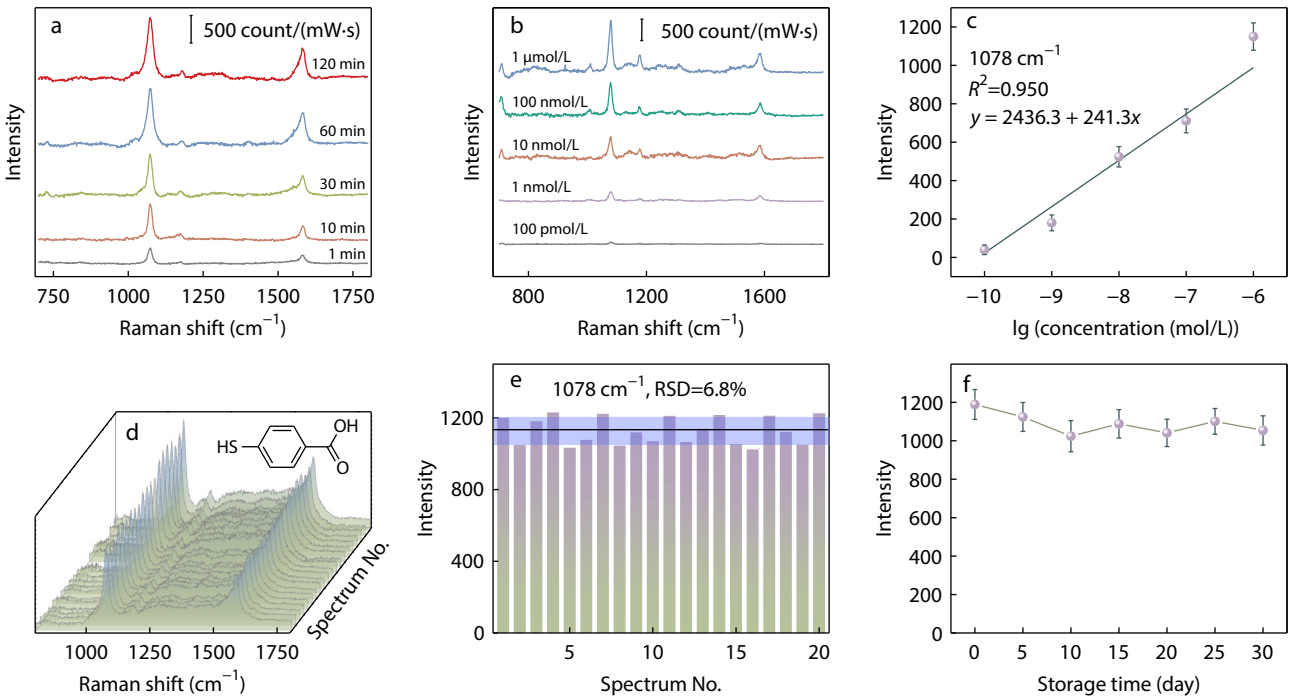

Fig. 3 (a) Effect of soaking time on response signal intensity of the flexible SERS substrate. (b) Raman spectra of 4-MBA molecules from 1 μmol/L to 100 pmol/L on the PDMS-based SERS substrates. (c) Linear calibration plot of SERS intensity and the concentration of 4-MBA ranging from 1 μmol/L to 100 pmol/L. (d) SERS signal of 4-MBA (1 μmol/L) randomly recorded at 20 points from PDMS-based SERS substrates and (e) the corresponding intensity distribution at the 1078 cm^{-1} band. (f) Relationship between the Raman intensity at band 1078 cm^{-1} and the storage time.

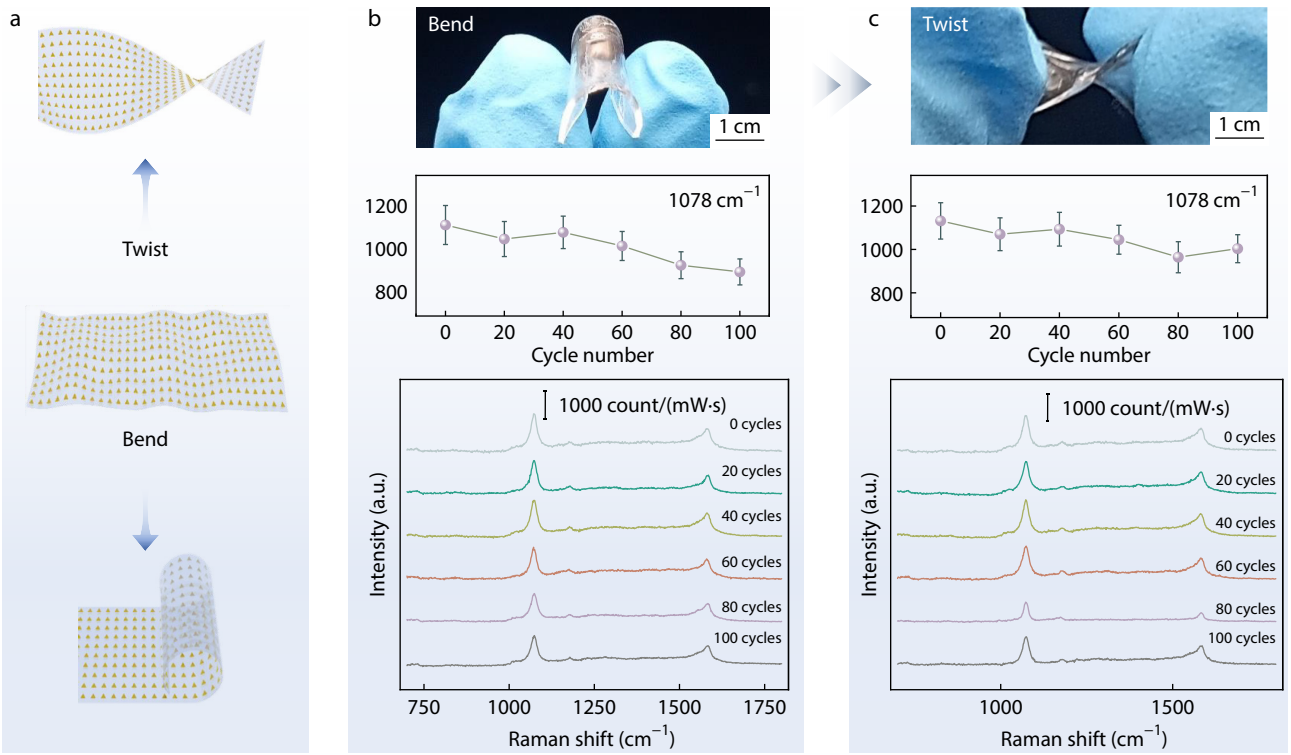

Fig. 4 (a) Schematic illustration of the durability test as mechanical stimuli of the flexible PDMS hybrid films. Comparative SERS intensity and Raman spectra (b) after the bending in half of the flexible SERS substrate, and (c) after the torsion to about 180° of the flexible SERS substrates for 100 cycles.

https://doi.org/10.1007/s10118-025-3373-z

An important assessment for evaluating an ideal flexible SERS substrate is its mechanical stability, which is vital for practical applications. The mechanical durability of the PDMS hybrid films was revealed using different mechanical deformations, including bending and torsion, for 100 cycles (Fig. 4a). For the bending and torsion tests, the PDMS hybrid films were bent in half and twisted to approximately 180° (Figs. 4b and 4c), respectively. Following mechanical stress exposure (bending/torsion cycles), the structural integrity of the Au nanoparticle assemblies on the PDMS surfaces remained preserved, as evidenced by SEM characterization of the post-deformation substrate surface (Fig. S8 in ESI). The resulting SEM analysis demonstrated that the PDMS hybrid films subjected to 100 bending or twisting cycles maintained their original configuration without detectable crack formation or material deterioration, thereby validating their exceptional mechanical and fatigue resistance. Periodic spectral monitoring at 20-cycle intervals (Figs. 4b and 4c) revealed <5% variation in 4-MBA (1 μmol/L) Raman signal intensity throughout 100 mechanical cycles relative to the undeformed controls. This mechanical resilience originates from the strong interfacial adhesion between the Au architectures and PDMS matrix, ensuring operational reliability in field-deployable sensing scenarios. Furthermore, the substrate incorporated a dual-function protective layer: an inert polymer brush coating prevented nanostructure dislodgement while permitting analyte permeation to the underlying plasmonic surfaces. This design provides SERS nanostructures with a robust connection to the flexible substrate while maintaining high sensitivity to the detected molecules, and ultimately realizes that the nanostructures and SERS signals remain virtually identical to their initial state after 100 bending cycles. For comparison, we provide a summary of the four key parameters of our flexible SERS substrate versus those of six recent representative flexible SERS

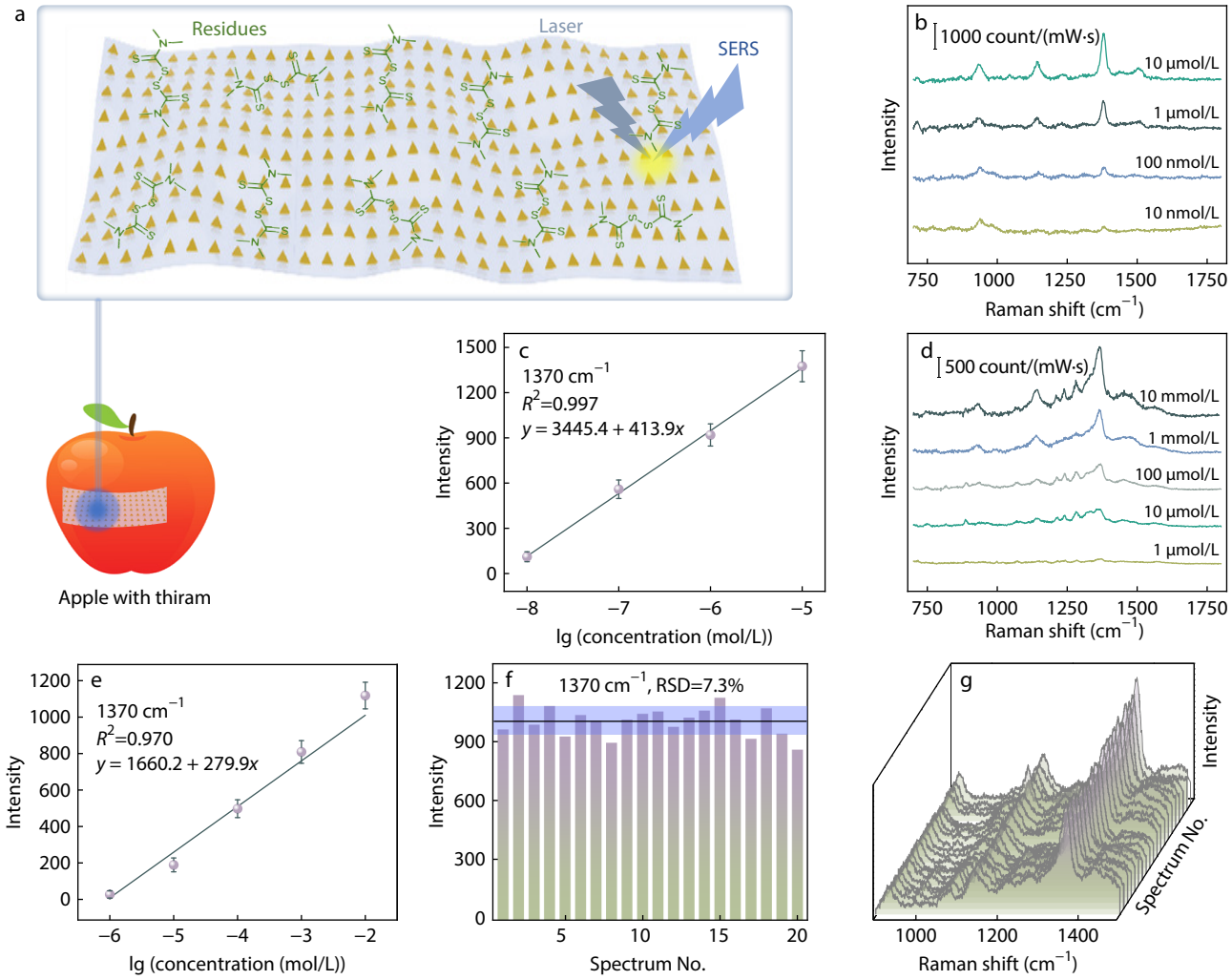

Fig. 5 (a) Illustration of the process and principles of detecting thiram molecules from apple skin using flexible SERS substrates; (b) Raman spectra of thiram molecules from the flexible hybrid film; (c) Linear calibration plot of Raman intensity and the immersion concentration of thiram ranging from 10 μmol/L to 10 nmol/L; (d) Raman spectra of thiram molecules from 10 mmol/L to 1 μmol/L recorded from the apple skin; (e) Linear calibration plot of SERS intensity versus the thiram concentration at 1078 cm^{-1}; (f, g) SERS signal of thiram (10 mmol/L) samples from randomly chosen points of the PDMS hybrid film and the corresponding intensity distribution at the 1078 cm^{-1} band (the average value is plotted with the black line, and the navy region indicates the intensity of the variation of ± 7.3%).

https://doi.org/10.1007/s10118-025-3373-z

substrates (Table S1 in ESI).[32–37] It is evident that our flexible SERS substrate exhibits a combination of comprehensive advantages.

Owing to its distinct flexibility, transparency, and good mechanical stability, the PDMS hybrid film is advantageous for the collection of analytes on various non-planar surfaces. Here, "press-peel off" process was employed to achieve the direct, rapid, and sensitive detection of thiram molecules on apple skin. The mechanism of the PDMS hybrid films for the "press-peel off" detection of thiram molecules on apple skin is illustrated in Fig. 5(a) (see ESI for experimental details). Although thiram molecules with the same concentration showed weaker Raman intensities when detected by "press-peel off" analysis (Figs. 5b and 5c), LOD values as low as 1 μmol/L were determined for thiram (Fig. 5d) and bands at 1145 cm^{-1} (S—C—N stretching and CH_3 rocking) and 1370 cm^{-1} (C—N stretching and CH_3 rocking) can be distinctly observed. As shown in Fig. 5(e), a linear calibration curve was obtained (R^2 = 0.970), indicating that the films possessed reliable SERS effects for trace detection and displayed good SERS activity in practical analysis.

To further explore the uniformity of trace detection in a real analyte, the SERS intensities across the PDMS hybrid films were measured from 20 randomly chosen points. Arguably, with a relative standard deviation of 7.3%, there was no significant change in the SERS intensities at the different points (Figs. 5f and 5g). Furthermore, a systematic evaluation of the SERS effects of residual probe molecules on diverse agricultural products was conducted using a flexible SERS substrate (Fig. S9 in ESI). The results revealed distinct SERS response characteristics across the three representative agricultural specimens: apple, banana, and cucumber. Notably, the signal intensity exhibited high consistency between the apple and banana surfaces, whereas a statistically significant attenuation in SERS intensity was observed for the cucumber surface. This differential SERS enhancement behavior is preliminarily attributed to variations in interfacial roughness, which may modulate the localized electromagnetic field distribution and surface plasmon resonance coupling efficiency at the substrate-probe interface. The results demonstrated that the PDMS hybrid films possessed good mechanical durability and homogeneous SERS activity for trace detection.

CONCLUSIONS

In summary, this study demonstrates a scalable assembly-transfer protocol for fabricating mechanically compliant PDMS-Au hybrid films with integrated SERS functionality. The plasmonic substrate exhibited exceptional analytical performance, including a 1.76×10^8 surface enhancement factor and 7.3% signal uniformity for 4-MBA detection, enabled by dense Au NP packing with controlled interparticle spacing. Environmental durability testing revealed 95% signal retention after 30-day ambient storage, whereas cyclic mechanical loading (100 bending/torsion cycles) induced <5% signal variation, confirming robust interfacial adhesion between the Au architectures and the PDMS matrix. Field validation using a non-destructive press-adhesion technique successfully detected thiram residues on apple surfaces at a concentration of 1 μmol/L, highlighting its practical applicability for agricultural monitoring. This methodology bridges laboratory-scale sensitivity with real-world deployability, and offers a versatile platform for on-site contaminant screening in food safety systems.

Conflict of Interests

The authors declare no interest conflict.

Electronic Supplementary Information

Electronic supplementary information (ESI) is available free of charge in the online version of this article at http://doi.org/10.1007/s10118-025-3373-z.

Data Availability Statement

The related data of this paper should not be shared, and can be obtained from the authors upon reasonable reasons. The author's contact information: Hzk@fosu.edu.cn.

ACKNOWLEDGMENTS

This work was financially supported by the National Natural Science Foundation of China (Nos. 22401045 and 22301037) and Natural Science Foundation of Guangdong Province (No. 2022A1515110867).

REFERENCES

1 PayneSturges, D.; Cohen, J.; Castorina, R.; Axelrad, D. A.; Woodruff, T. J. Evaluating cumulative organophosphorus pesticide body burden of children: a national case study. *Environ. Sci. Technol.* **2009**, *43*, 7924–7930.
2 Martínez Vidal, J. L.; Plaza-Bolaños, P.; Romero-González, R.; Garrido Frenich, A. Determination of pesticide transformation products: a review of extraction and detection methods. *J. Chromatogr. A* **2009**, *1216*, 6767–6788.
3 Xu, M. L.; Gao, Y.; Han, X. X.; Zhao, B. Detection of pesticide residues in food using surface-enhanced Raman spectroscopy: A Review. *J. Agric. Food Chem.* **2017**, *65*, 6719–6726.
4 Jia, K.; Xie, J.; He, X.; Zhang, D.; Hou, B.; Li, X.; Zhou, X.; Hong, Y.; Liu, X. Polymeric micro-reactors mediated synthesis and assembly of Ag nanoparticles into cube-like superparticles for SERS application. *Chem. Eng. J.* **2020**, *395*, 125123.
5 Parvathi, V. P.; Parimaladevi, R.; Sathe, V.; Umadevi, M. Environmental photochemistry by plasmonic semiconductor decorated GO nanocomposites: SERS detection and visible light driven degradation of aromatic dyes. *Appl. Surf. Sci.* **2019**, *473*, 864–872.
6 Nie, S.; Emory, S. R. Probing single molecules and single nanoparticles by surface-enhanced Raman scattering. *Science* **1997**, *275*, 1102.
7 Fang, Y.; Seong, N. H.; Dlott, D. D. Measurement of the distribution of site enhancements in surface-enhanced Raman scattering. *Science* **2008**, *321*, 388.
8 Shao, M.; Ji, C.; Tan, J.; Du, B.; Zhao, X.; Jing, Y.; Man, B.; Xu, K.; Zhang, C.; Li, Z. Ferroelectrically modulate the Fermi level of graphene oxide to enhance SERS response. *Opto-Electron. Adv.* **2023**, *6*, 230094.
9 Liu, Y.; Qiao, S.; Fang, C.; He, Y.; Sun, H.; Liu, J.; Ma, Y. A highly

sensitive LITES sensor based on a multi-pass cell with dense spot pattern and a novel quartz tuning fork with low frequency. *Opto-Electron. Adv.* **2024**, *7*, 230230.
10 Zhu, K.; Zhou, T.; Chen, P.; Zong, S. F.; Wu, L.; Cui, Y. P.; Wang, Z. Y. Long-lived SERS matrix for real-time biochemical detection using "Frozen" transition state. *ACS Sens.* **2023**, *8*, 3360–3369.
11 Peng, R.; Zhang, T. T.; Wang, S. Y.; Liu, Z. J.; Pan, P.; Xu, X. T.; Song, Y. X.; Liu, X. Y.; Yan, S.; Wang, J. S. Self-assembly of strain-adaptable surface-enhanced Raman scattering substrate on polydimethylsiloxane nanowrinkles. *Anal. Chem.* **2024**, *96*, 10620–10629.
12 Xie, L. P.; Zeng, H.; Zhu, J. X.; Zhang, Z. L.; Sun, H. B.; Xia, W.; Du, Y. N. State of the art in flexible SERS sensors toward label-free and onsite detection: from design to applications. *Nano Res.* **2022**, *15*, 4374–4394.
13 Zhao, X.; Cui, C. Y.; Ma, L.; Ding, Z. H.; Hou, J. S.; Xiao, Y. X.; Liu, B. W.; Qi, B. J.; Zhang, J. H.; Lu, X. L.; Wei, J. J.; Watanabe, S.; Hao, N. J. Acoustofluidic one-step production of plasmonic Ag nanoparticles for portable paper-based ultrasensitive SERS detection of bactericides. *J. Colloid Interface Sci.* **2024**, *673*, 426–433.
14 Zhang, X.; Yao, J.; Gong, X.; Sun, J.; Wang, R.; Wang, L.; Liu, L.; Huang, Y. Paper electrophoretic enrichment-assisted ultrasensitive SERS detection. *Food Chem.* **2024**, *434*, 137416.
15 Alawadhi, H.; Alnaqbi, M. A.; Ramachandran, K.; Columbus, S.; Daoudi, K.; Chidambaram, S.; El Khakani, M. A.; Gaidi, M. Trace-level sensing of food toxins by flexible and cost-effective SERS sensors fabricated by pulsed-laser-deposition of gold nanoparticles on polycarbonate matrix. *Surf. Interfaces* **2023**, *40*, 103016.
16 Meng, S. J.; Liang, J. X.; Jia, W. M.; Zhang, P.; Su, Q.; Wang, C. J.; An, L. L.; Chen, L. H.; Wang, Y. B. Metal-free and flexible surface-enhanced Raman scattering substrate based on oxidized carbon cloth. *Carbon* **2022**, *189*, 152–161.
17 Barveen, N. R.; Chinnapaiyan, S.; Wang, T. J.; Huang, C. H. Photochemical decoration of gold nanoparticles on MoS2 nanoflowers grafted onto the flexible carbon cloth as a recyclable SERS sensor for the detection of antibiotic residues on curved surfaces. *Chemosphere* **2024**, *346*, 140677.
18 Wang, B. X.; Duan, G. Y.; Xu, W.; Xu, C. Y.; Jiang, J. Y.; Yang, Z. C.; Wu, Y. K.; Pi, F. W. Flexible surface-enhanced Raman scatting substrates: recent advances in their principles, design strategies, diversified material selections and applications. *Crit. Rev. Food Sci. Nutr.* **2024**, *64*, 472–516.
19 Liu, H. Q.; He, Y. N.; Cao, K. Z. Flexible surface-enhanced Raman scattering substrates: A review on constructions, applications, and challenges. *Adv. Mater. Interfaces* **2021**, *8*, 15.
20 Liu, X. F.; Ma, J. M.; Jiang, P. F.; Shen, J. L.; Wang, R. W.; Wang, Y.; Tu, G. L. Large-scaleflexible surface-enhanced Raman scattering (SERS) sensors with high stability and signal homogeneity. *ACS Appl. Mater. Interfaces* **2020**, *12*, 45332–45341.
21 Ma, Y.; Chen, Y.; Tian, Y.; Gu, C.; Jiang, T. Contrastive study of in situ sensing and swabbing detection based on SERS-active gold nanobush-PDMS hybrid film. *J. Agric. Food Chem.* **2021**, *69*, 1975–1983.
22 Markin, A. V.; Arzhanukhina, A. I.; Markina, N. E.; Goryacheva, I. Y. Analytical performance of electrochemical surface-enhanced Raman spectroscopy: a critical review. *TrAC-Trends Anal. Chem.* **2022**, *157*, 116776.
23 Li, M.; He, X.; Wu, C.; Wang, L.; Zhang, X.; Gong, X.; Zeng, X.; Huang, Y. Deep learning enabled SERS identification of gaseous molecules on flexible plasmonic MOF nanowire films. *ACS Sens.* **2024**, *9*, 979–987.
24 Yi, S.; Yang, M.; Yu, Y.; Li, Z.; Zhang, D.; Han, F.; Grishko, A.; Li, Y.; Qin, Q.; Zhou, B. Highly sensitive flexible SERS substrates with a sandwich structure for rapid detection of trace pesticide residues. *Appl. Surf. Sci.* **2024**, *654*, 159455.
25 Song, X.; You, X.; Ren, X.; Zhang, X.; Tang, D.; Li, X. Vertically aligned Ag-decorated MoS2 nanosheets supported on polyvinyl alcohol flexible substrate enable high-sensitivity and self-cleaning SERS devices. *J. Environ. Chem. Eng.* **2023**, *11*, 109437.
26 Park, S.; Lee, J.; Ko, H. Transparent and flexible surface-enhanced Raman scattering (SERS) sensors based on gold nanostar arrays embedded in silicon rubber film. *ACS Appl. Mater. Interfaces* **2017**, *9*, 44088–44095.
27 Liu, P.; Peng, J.; Chen, Y.; Liu, M.; Tang, W.; Guo, Z.-H.; Yue, K. A general and robust strategy for in-situ templated synthesis of patterned inorganic nanoparticle assemblies. *Giant* **2021**, *8*, 100076.
28 Peng, J.; Liu, P.; Chen, Y.; Guo, Z. H.; Liu, Y.; Yue, K. Templated synthesis of patterned gold nanoparticle assemblies for highly sensitive and reliable SERS substrates. *Nano Res.* **2022**, *16*, 5056–5064.
29 Chen, M. M.; Zhang, J. X.; Zhu, X. J.; Liu, Z. H.; Huang, J. L.; Jiang, X. C.; Fu, F. F.; Lin, Z. Y.; Dong, Y. Q. Hybridizing silver nanoparticles in hydrogel for high-performance flexible SERS chips. *ACS Appl. Mater. Interfaces* **2022**, *14*, 26216–26224.
30 Pang, X.; He, Y.; Jung, J.; Lin, Z. 1D nanocrystals with precisely controlled dimensions, compositions, and architectures. *Science* **2016,** *353*, 1268–1272.
31 Pang, X.; Zhao, L.; Han, W.; Xin, X.; Lin, Z. A general and robust strategy for the synthesis of nearly monodisperse colloidal nanocrystals. *Nat. Nanotechnol.* **2013**, *8*, 426–431.
32 Li, Z.; Zhai, L.; Zhang, Q.; Zhai, W.; Li, P.; Chen, B.; Chen, C.; Yao, Y.; Ge, Y.; Yang, H.; Qiao, P.; Kang, J.; Shi, Z.; Zhang, A.; Wang, H.; Liang, J.; Liu, J.; Guan, Z.; Liao, L.; Neacșu, V. A.; Ma, C.; Chen, Y.; Zhu, Y.; Lee, C. S.; Ma, L.; Du, Y.; Gu, L.; Li, J. F.; Tian, Z.Q.; Ding, F.; Zhang, H. 1T'-transition metal dichalcogenide monolayers stabilized on 4H-Au nanowires for ultrasensitive SERS detection. *Nat. Mater.* **2024,** *23*, 1355–1362.
33 Kim, J.; Kim, J. M.; Choi, K.; Park, J. E.; Nam, J. M. Open cross-gap gold nanocubes with strong, large-area, symmetric electromagnetic field enhancement for on-particle molecular-fingerprint raman bioassays. *J. Am. Chem. Soc.* **2024**, *146*, 14012–14021.
34 Liu, X.; Wang, J.; Tang, L.; Xie, L.; Ying, Y. Flexible plasmonic metasurfaces with user-designed patterns for molecular sensing and cryptography. *Adv. Funct. Mater.* **2016**, *26*, 5515–5523.
35 Lin, H. Y.; Chen, W. R.; Lu, L. C.; Chen, H. L.; Chen, Y. H.; Pan, M.; Chen, C. C.; Chen, C.; Yen, T. H.; Wan, D. Direct thermal growth of gold nanopearls on 3D interweaved hydrophobic fibers as ultrasensitive portable SERS substrates for clinical applications. *Small* **2023**, *19*, 2207404.
36 Xu, Z.; Erinomo, A. M.; Dan, Z.; Qin, F.; Chang, H. Flexible SERS substrates with gradient porous Cu structure dealloying from the thermal diffusion couples of Al/Cu stacking foils. *Chem. Eng. J.* **2024**, *490*, 151871.
37 Kong, S. M.; Shin, D.; Oh, J. W.; Park, H.; Lee, J. S.; Won, N.-I.; Na, Y. H. One-pot platform for the collection and detection of nanoparticles: flexible surface-enhanced Raman scattering (SERS) substrates with nano-pore structure. *Chem. Eng. J.* **2023**, *471*, 144753.

https://doi.org/10.1007/s10118-025-3373-z